

FULL PAPER

Investigation of enantiomeric separation of tiletamine drug using computational chemistry methods

Nabi Javadi*,  | Hossein Fakhraian *Department of Chemistry, Faculty of Science, Imam Hossein University, Tehran, Iran*

In this paper, the ability of organic reagents such as the succinate, oxalate, maleate, fumarate, adipate, glutarate, suberate, and pimelate anions in separation of different enantiomer form of tiletamine compound (R&S) is investigated using the density functional theory method (DFT). Our findings showed that the conglomerate crystal of tiletamine is formed in the presence of succinate, oxalate, fumarate, and maleate organic reagents. Moreover, the racemic mixture of tiletamine is formed in the presence of adipate, glutarate, suberate, and pimelate anions. According to the thermodynamic parameters of tiletamine-organic anion interactions, it is revealed that, in comparison to chloroform, internal thermal energy, enthalpy, and Gibbs free energy become more positive in the presence of ethanol and water solvents indicating the enfeeble effect of solvent polarity on enantiomer separation. Also, it should be noted that the existence of carbon chain lengths greater than three atoms in the organic anion is not suitable for enantiomeric separation. The natural bond orbital (NBO) and Atom In Molecules (AIM) results show that tiletamine nitrogen atom is the primary site of interaction with the oxalate, succinate, fumarate, and maleate anions.

***Corresponding Author:**

Nabi Javadi

E-mail: Nabi250@gmail.com

Tel.: +982177104930

KEYWORDS

Tiletamine; enantiomer separation; thermodynamic parameters; conglomerate crystal; organic reagent.

Introduction

The purification of enantiomer compounds has become an important subject of science because of different pharmacological and toxicological effects that enantiomers exert in different parts of human bodies [1]. Therefore, the studies on the enantiomeric purification method have been increased in pharmaceutical, food, and military industries [2-4]. These studies are focused on the stereoselective crystallization methods such as asymmetric synthesis, preferential

crystallization, and chromatography [5-7]. The preferential crystallization is more economical because of high cost of instrumental methods and drawback of asymmetric synthesis [8]. In this method, the chiral separation occurred in the presence of chiral or achiral agent such as chiral polymeric surface, acid, and base achiral reagents [9, 10].

Enantiomer compounds include stereoisomer that shows different properties in living organism [11]. These compounds form two types of crystal including

homochiral crystal as a conglomerate and heterochiral crystal as a racemic mixture or racemate. The conglomerate form of chiral compounds is produced in the presence of strong homochiral interactions [12]. The types of functional groups and crystallization condition are an important factor increasing the strength of homochiral interaction. The effect of functional groups of enantiomer compound and solvent polarity on the separation of asparagine, ibuprofen, and atenolol compounds has been previously studied [13]. It has been found that the amine and carboxylate acid functional groups of enantiomer compounds increased the possibility of conglomerate formation. As well as, in the presence of water solvent, the asparagine, ibuprofen and atenolol compounds formed the conglomerate, racemic and solid solution respectively.

The purification of the 1-phenylethylamine compound has been investigated by using achiral dicarboxylic acids reagents. The obtained results indicate that the hydrogen succinate formed the conglomerate crystal of 1-phenylethylamine. Also, the racemic form of 1-phenylethylamine has been produced in the presence of hydrogen malonate and hydrogen phthalate reagents [14]. These results showed that the presence of hydrogen bond networks have an important effect on the conglomerate crystal formation of 1-phenylethylamine. The feasibility of conglomerate crystal formation of medetomidine using the oxalate, chloride, bromide, and iodide anions in the presence of ethanol and 2-propanol solvents has also been investigated [15]. It has been found that oxalate anion gives the pure form of medetomidine and the stability of conglomerate crystal of medetomidine increased in the presence of ethanol. Therefore, it is indicated that solvent polarity is an important factor controlling the purification of enantiomer compound.

Recently, computational chemistry methods were used to investigate the

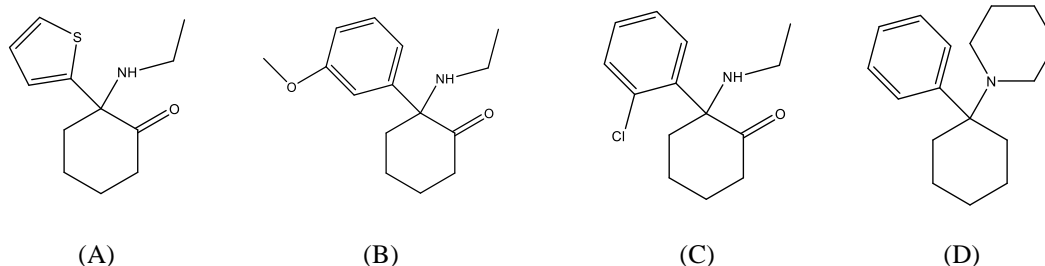
separation of enantiomer compound. Selective complexation between α , β , and γ form of cyclodextrin with cathinone has been previously investigated using DFT calculation and MD simulations [16]. The obtained results indicated that hydrogen bond formation is the main interaction in the cyclodextrin-cathinone complex. Furthermore, the stability of γ -cyclodextrin-cathinone complex is more than α and β forms and the complex stability in gas phase is more than in water, chloroform, and methanol.

The ability of carbon nanotubes (CNTs) in the separation of R-/S-ibuprofen isomers has also been investigated using DFT calculations [17]. The obtained results indicated that the R and S form of ibuprofen have stronger interaction with inner side of CNTs. Moreover, the strength of interaction in the S-ibuprofen is more than in the R-ibuprofen which shows that the encapsulation of drugs molecules into CNTs increased the CNTs ability in the purification of ibuprofen compound. Additionally, they found that the solvent cannot affect the strength of interaction between CNTs and the R-/S-ibuprofen isomers. The possibility of conglomerate crystal formation of medetomidine and ketamine ($C_{13}H_{16}ClNO$) salts in the presence of acidic achiral reagents have been theoretically studied [18-21]. Based on the obtained results, the hydrogen bond formation between the nitrogen atoms of enantiomers and the oxygen atom of acidic reagents is introduced as the primary sites of interaction that increased the possibility of conglomerate crystal formation. The energy analysis results demonstrated that in the case of medetomidine and ketamine salts, the conglomerate crystal is formed in the presence of oxalic and fumaric acid reagents, respectively. Likewise, racemic mixture is formed in the presence of formic, carbonic, acetic, and hydrochloride acids reagents.

Tiletamine ($C_{12}H_{17}NOS$) was synthesized by Parke-Davis in the 1960s with similar

structure to ketamine and phencyclidine ($C_{17}H_{25}N$) compounds. This compound possesses a higher psychotomimetic, and amnestic properties in comparison to ketamine (the chemical structure of

tiletamine, methoxetamine ($C_{15}H_{21}NO_2$), ketamine and phencyclidine are depicted in Scheme 1 [22, 23].



SCHEME 1 The chemical structure of (A) tiletamine, (B) methoxetamine, C) ketamine, and (D) phencyclidine

Tiletamine is synthesized as a racemic mixture including the R- and S enantiomers showing different biological effect on human body. Therefore, to examine the biological effect of the R- and S form of tiletamine on human body, the preparation of enantiopure form of the tiletamine is of great importance [24]. To date, a suitable method has not been conducted for enantiomer purification of tiletamine. In this study, the interaction between two tiletamine enantiomers and achiral organic acid anions including the succinate, oxalate, maleate, fumarate, pimelate, suberate, glutarate, and adipate are investigated using quantum chemistry calculations. These kind of organic acid anions have been used to examine the effect of carbon chain length of organic anions on the formation of conglomerate crystal. In addition, the effects of solvents on the strength of interaction between the organic reagents and tiletamine are studied in the presence of solvents such as water, ethanol,

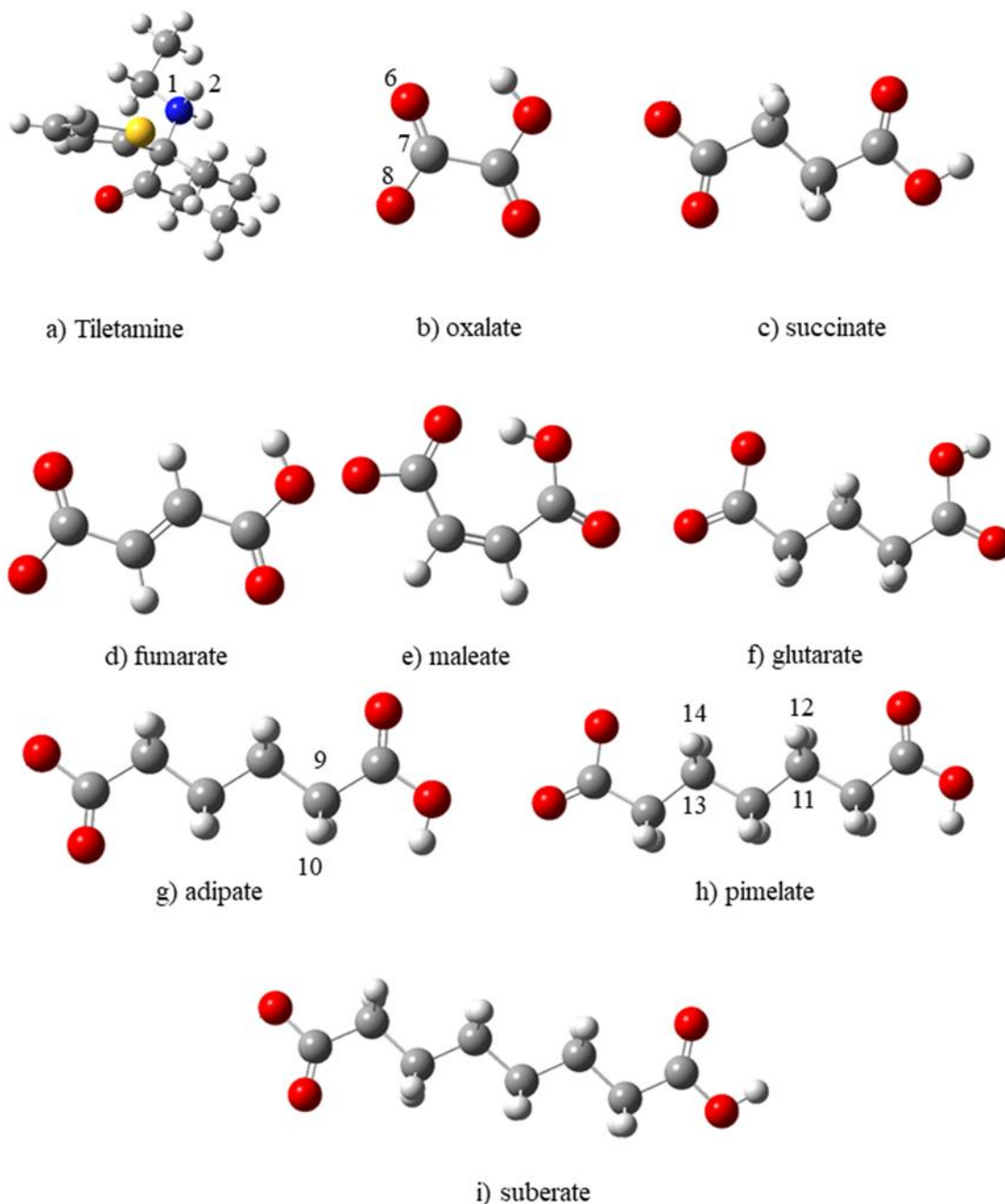
and chloroform. The structure of tiletamine and the organic achiral anions are shown in Scheme 2.

Computational details

The DFT calculations were used to investigate the interaction between the RR, SS, and RS enantiomeric forms of tiletamine with the organic reagent using the M06-2X function at the 6-311g(d, p) level of theory by employing Gaussian 09 software [25-27]. The optimized structures were confirmed using the vibrational frequency calculations with no imaginary frequencies. Also, the internal energy (ΔE), enthalpy (ΔH), entropy (ΔS), and Gibbs energy (ΔG) of interaction were calculated using Equation (1):

$$\Delta X_{\text{interaction}} = X_{(\text{Tiletamine-achiral acidic reagent})} - (X_{(\text{Tiletamine})} + X_{(\text{achiral acidic reagent})}) \quad (1)$$

Where, x= G, H, E, and S.



SCHEME 2 The molecular structures of (a) Tiletamine and organic reagent including (b) oxalate, (c) succinate, (d) fumarate, (e) maleate, (f) glutarate, (g) adipate, (h) pimelate, and (i) suberate anions

The effect of solvent polarity on different structures was studied by employing the PCM in the attendance of chloroform, ethanol, and water [28,29]. The natural bond orbital (NBO) analyses were made to explore the primary site of interaction between tiletamine and organic achiral anions [30]. Quantum theory of atoms in molecules (QTAIM) were employed to investigate the electron localization function (ELF), the

localized orbital locator (LOL), the noncovalent interaction (NCI), and the reduced density gradient (RDG) plots at the bond critical points (BCPs) which provide an insight about the strength and nature of interactions between the organic achiral reagents and tiletamine [31-33]. All of QTAIM analyses were calculated using Multi-WFN 3.7 program [34].

Results and discussion

Geometry analysis

The electrostatic surface potential (ESP) scheme for the tiletamine (Figure 1a) display that nitrogen atom of tiletamine is the best site for interaction with the carboxylate groups of organic reagents because of the more positive charge on this atom. The initial structure of tiletamine and organic achiral reagent are considered in the salt and anionic form, respectively. Likewise, the orientation of organic achiral reagents with respect to the initial structure of tiletamine salt is represented in Figure 1b. The $N_1 \cdots H_2$ and $O_8 \cdots H_2$ bond length are analyzed to investigate the strength of interaction between the organic anions and tiletamine salt enantiomers. The obtained results are listed in Table S1. The optimized structures of tiletamine-organic achiral reagent are represented in Figure S1. As demonstrated in

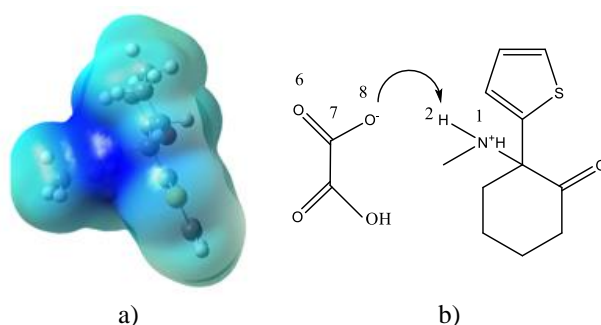


FIGURE 1 (a) The ESP presentation of tiletamine and (b) The direction of organic reagents with respect to the initial structure of tiletamine

According to the results, the moderately ionic hydrogen bonds are considered in the case of oxalate, fumarate, succinate, and maleate reagents. Therefore, it can be concluded that RR and SS forms of tiletamine shows more appropriate interaction in comparison to the RS form of tiletamine that increase the feasibility of conglomerate crystal formation. By comparing the $N_1 \cdots H_2$ bond length in the proximity of fumarate and maleate anions, it has been observed that cis isomer (malonate anion) have lower bond length in comparison

Figure S1, the hydrogen transfer are observed from the nitrogen atom of tiletamine to the oxygen atom of organic reagent that shows during the optimization of the initial salt form of tiletamine changed to the base form of tiletamine. Also, the oxalate, malate, fumarate, and succinate anions shows the strong interaction with the positive site of tiletamine whereas the adipate, glutarate, pimlate, and suberate anions formed the chelate structure around tiletamine enantiomers that can be attributed to the steric barrier of carbon chain length in these anions. Therefore, it can be concluded that the interaction intensity between tiletamine and organic achiral anions decreased with increasing in the carbon chain length between two carboxylate groups of the organic anions. The strong, moderately ionic, and weak dispersion hydrogen bonds are introduced based on the geometrical parameters such as bond length, bond angle, and bond energy [34].

to trans form of anion (fumarate anion). In addition, it is indicated that the $N_1 \cdots H_2$ bond length decrease with increase in alkyl chain length between carboxylate groups of adipate, glutarate, suberate, and pimlate anions.

Energy analysis

The interaction of achiral organic anions with tiletamine is studied using the interaction energy ($\Delta E_{\text{interaction}}$), as presented in Table 1.

TABLE 1 The obtained $\Delta E_{\text{interaction}}$ (kcal.mol⁻¹) of organic anions and TIL in the gas phase, ethanol, chloroform, and water at M06-2X/6-311G (d,p) level of theory

Structure	$\Delta E_{\text{interaction}}$ (Gas)	$\Delta E_{\text{interaction}}$ (Chloroform)	$\Delta E_{\text{interaction}}$ (Ethanol)	$\Delta E_{\text{interaction}}$ (Water)
RR-Oxalate	-16.11	-22.84	-22.86	-22.77
SS- Oxalate	-26.88	-33.88	-32.99	-32.85
RS- Oxalate	-21.03	-26.96	-26.56	-26.40
RR-Succinate	-24.85	-26.10	-24.12	-23.79
SS- Succinate	-30.46	-33.89	-32.06	-31.76
RS- Succinate	-25.24	-26.04	-24.45	-24.10
RR-Fumarate	-27.87	-30.20	-28.99	-28.70
SS- Fumarate	-34.59	-37.95	-36.88	-36.60
RS- Fumarate	-32.67	-33.44	-31.68	-31.29
RR-Maleate	-29.57	-30.46	-27.53	-27.14
SS- Maleate	-36.45	-38.44	-36.15	-35.77
RS- Maleate	-29.30	-29.00	-26.03	-26.13
RR-Glutarate	-13.02	-18.93	-18.12	-17.99
SS- Glutarate	-1.71	-9.53	-8.92	-8.83
RS- Glutarate	-15.96	-20.62	-19.45	-19.26
RR-Adipate	-19.46	-18.29	-15.97	-15.59
SS- Adipate	-32.37	-28.61	-26.27	-25.78
RS- Adipate	-24.75	-24.55	-22.90	-22.53
RR-Pimelate	-24.10	-23.83	-20.23	-19.83
SS- Pimelate	-20.82	-21.90	-18.50	-18.13
RS- Pimelate	-22.89	-23.04	-19.95	-19.53
RR-Suberate	-13.61	-15.50	-13.72	-13.53
SS- Suberate	-16.46	-18.58	-17.08	-16.84
RS- Suberate	-15.19	-17.94	-16.81	-16.63

The interaction energy of oxalate, fumarate, succinate, and malate reagents with the SS form of tiletamine is higher than the RR and RS enantiomeric forms of tiletamine. By increasing the carbon chain length between two carboxylate groups of glutarate, suberate, pimelate and adipate anions, the interaction energy of the RS form of tiletamine increases. By comparing the tiletamine-organic achiral reagents interaction energy, it is indicated that the interaction energy increased in the proximity of oxalate, fumarate, and succinate anions. Besides, the increment in the interaction energy in the chloroform proximity is more than water and ethanol that indicates the non-polar solvents is better for conglomerate crystal formation.

The interaction ability of organic anions and tiletamine is examined using the energy

difference between the interaction energy in SS-X (X= oxalate, succinate, fumarate, and maleate anions) and the RS-X ($\Delta\Delta E$) is calculated and reported in Table 2. According to our findings, in the presence of oxalate, succinate, fumarate, and maleate anions, it has been observed that maleate and oxalate show greater difference in the interaction energy ($\Delta\Delta E$) in comparison to other reagents. It is shown that in the imidazolium based ionic liquids with maleate anion; the anion with ring equilibrium structure gives lower interaction energy in comparison to open structure of anion because of the formation of intermolecular hydrogen bonds [36]. The maleate anions give the open structure in the interaction with different enantiomeric forms of tiletamine that this result is in agreement with the previously results [36].

TABLE 2 The energy difference between the interaction energy in the best form(s) of enantiomers (RR and SS) with the RS form of tiletamine in gas, ethanol, water, and chloroform (in kcal.mol⁻¹)

Compound	$\Delta\Delta E$ (gas)	$\Delta\Delta E$ (chloroform)	$\Delta\Delta E$ (ethanol)	$\Delta\Delta E$ (water)
Oxalate	-5.85	-6.92	-6.43	-6.45
Succinate	-5.22	-7.85	-7.61	-7.66
Fumarate	-1.92	-4.51	-5.2	-5.31
Maleate	-7.15	-9.44	-10.12	-9.64

The thermodynamic parameters in the tiletamine-organic achiral acid anions interaction were obtained (see Table S2). In addition, the thermodynamic diagrams used for better comparison between thermodynamic parameters in gas phase and in the proximity of ethanol, water, and chloroform (Figure 2). On the basis of thermodynamic results, the tiletamine-organic achiral reagent interactions are exothermic and the enthalpy value for these interactions in the proximity of the oxalate, fumarate, succinate, and maleate reagents is more than other organic achiral anions.

Furthermore, based on our findings, with increasing the carbon chain length between two carboxylate groups of the anions, the enthalpy and Gibbs free energy of the tiletamine-X interactions (X= glutarate, pimelate, adipate, and suberate reagents) decreased. This result indicates that steric barrier of carbon chain length of anions has a negative effect on the ability of conglomerate crystal formation. The value of thermodynamic parameters in the presence chloroform (non-polar solvent) is more than ethanol and water (polar solvent). Therefore, it can be concluded that the ability of organic anions for interaction with tiletamine decreased in polar environment.

NBO analysis

The NBO analysis was used to examine the strength of charge transfer at the primary site of interaction between tiletamine and organic achiral anions (Table S3).

According to the obtained results, the N₁...H₂ and H₂...O₆ is the primary site of interaction between tiletamine and organic anions. Moreover, it is indicated that the stabilization energy for interactions between the SS form of tiletamine and the oxalate, succinate, maleate, and fumarate anions is higher than the interaction between tiletamine and other organic achiral anions. The Lp_{N1} → Lp*_{H9} stabilization energy decreased by increasing the carbon chain length of the adipate glutarate, suberate, and pimelate anions that show the lower interaction ability of these organic anions with different form of tiletamine compound. These results are in agreement with the previous results that indicate the negative effect of steric barrier of adipate, glutarate, suberate, and pimelate anions in the conglomerate crystal formation of the tiletamine compound.

QTAIM Analysis

The interaction between the succinate, oxalate, fumarate, and maleate reagents with the SS form of tiletamine compound are investigated using the ELF and LOL diagrams (Figure 3). As depicted in Figure 3, electrons are localized between the N₁ and H₂ atoms of the SS form of TIL and O₈ atom of organic reagents that confirm the N-H...O interaction between the TIL and organic anions. Also, the high value of ELF and LOL between the H₂ atom of the SS form of tiletamine and the O₈ atom of organic anions confirms the strong interaction between these atoms. Therefore, it can be concluded that the N-H...O

interaction is the primary site of interaction between tiletamine and organic achiral anions. These results confirmed the high ability of succinate, oxalate, fumarate, and maleate in the interaction with effective site

of SS form off tiletamine and were in agreement with the previous results. In addition, N-H...O interaction was not seen in the case of other organic achiral reagents.

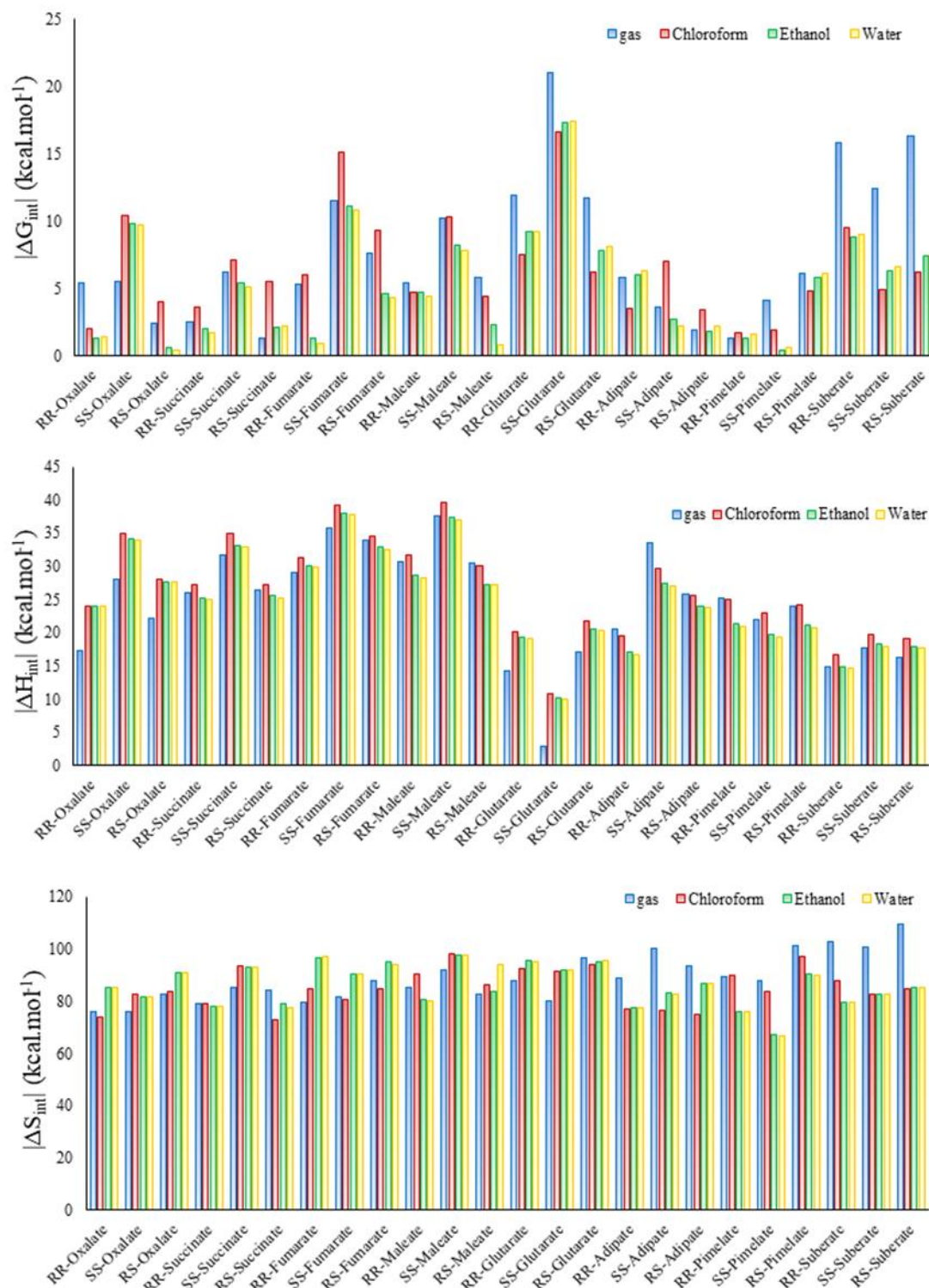


FIGURE 2 Thermodynamic diagram of interaction between organic reagents and tiletamine in gas phase, Ethanol, chloroform, and water

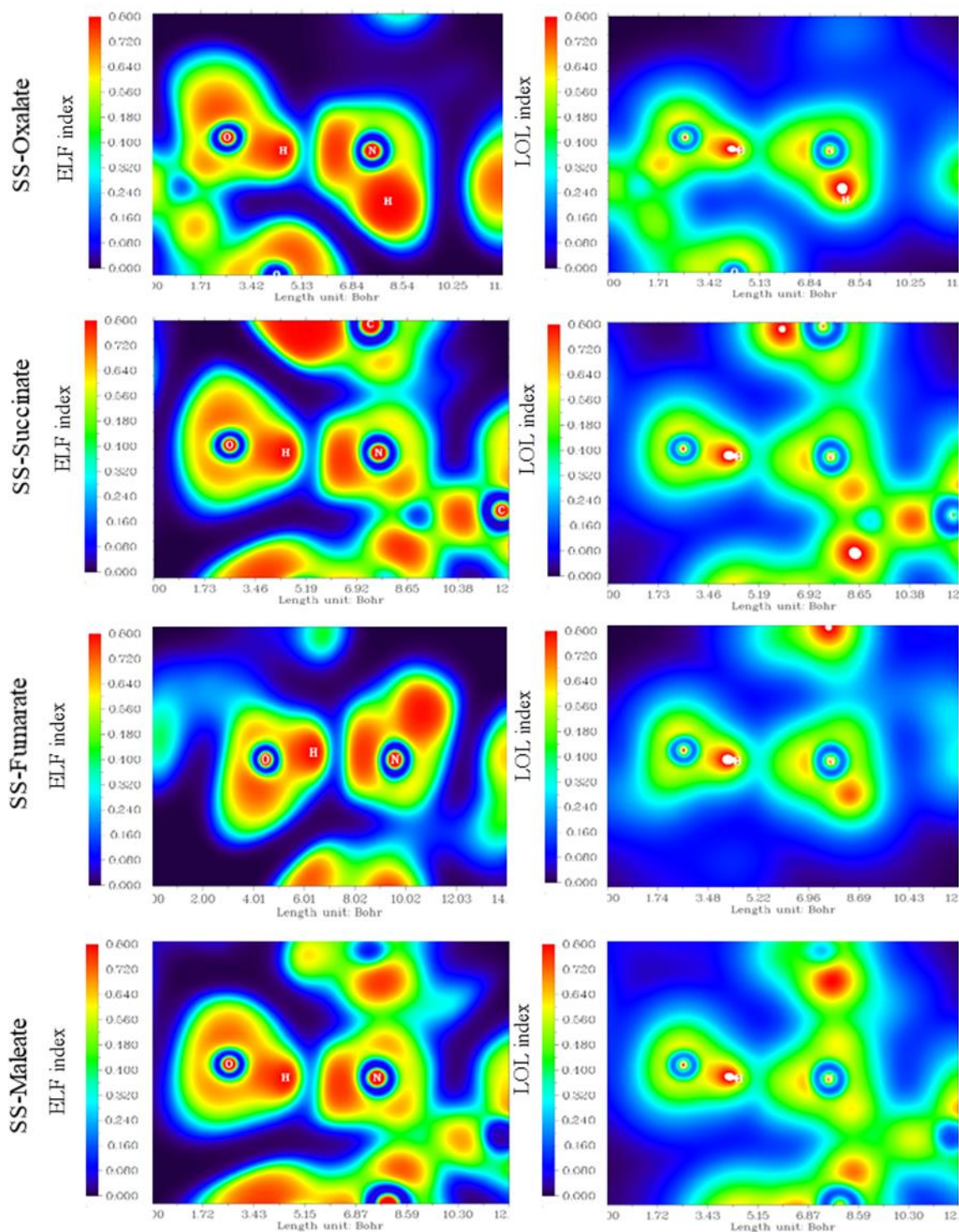


FIGURE 3 The LOL and ELF diagram of the interaction between SS form of tiletamine and the succinate oxalate, maleate, and fumarate reagents

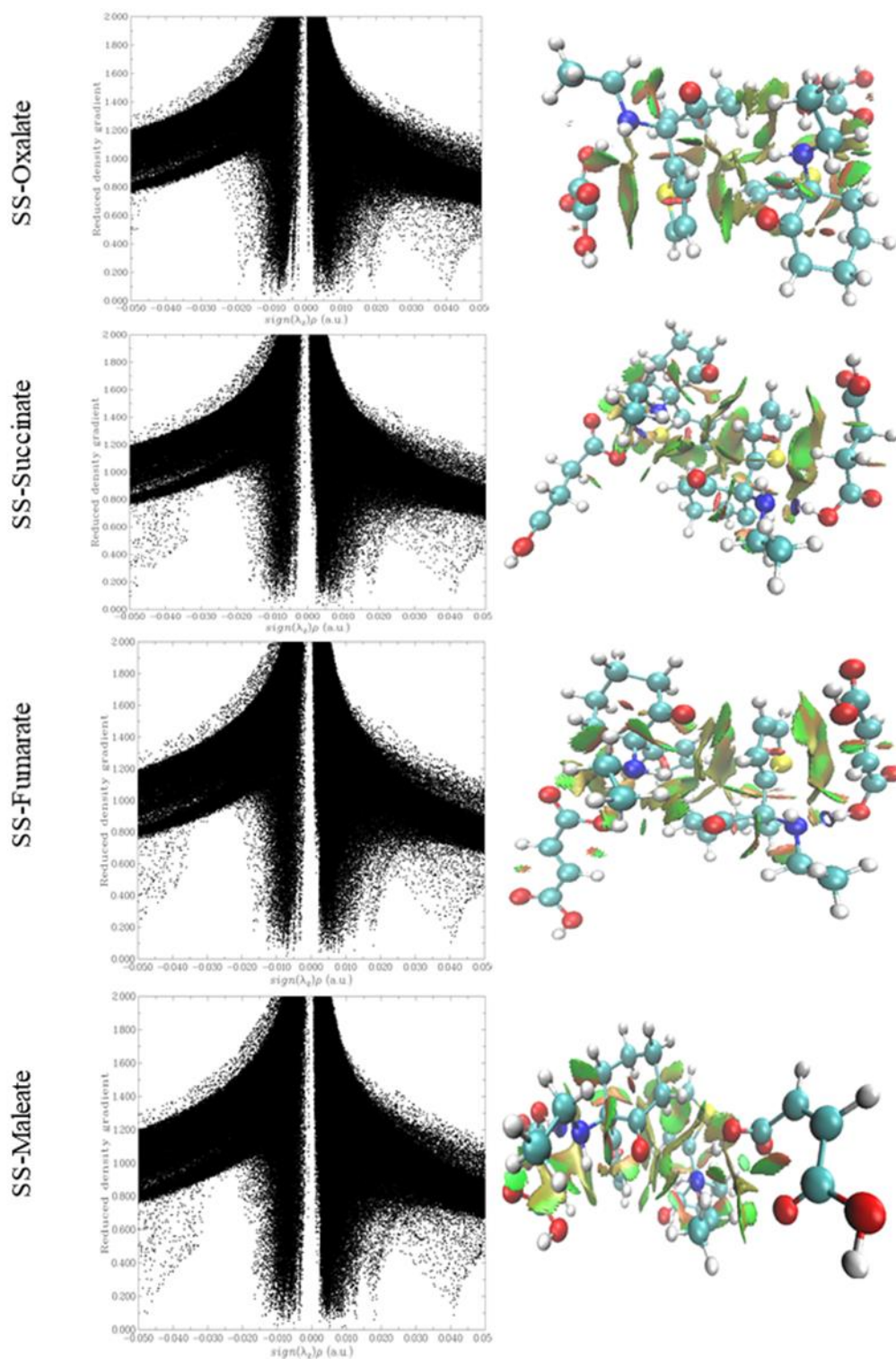


FIGURE 4 The 2D-NCI and 3D NCI plots of the interaction between SS form of tiletamine and the succinate, oxalate, maleate, and fumarate anions

The NCI and RDG diagrams give a qualitative knowledge about the essence of interaction between the organic achiral anions and SS form of tiletamine. The 2D-NCI and 3D NCI plots for the interaction between oxalate, succinate, fumarate, and maleate

anions and SS form of tiletamine are represented in Figure 4. In the 3D-NCI diagram, the red, green, and blue color-filled isosurfaces represent the mentioned interactions.

According to the results, the hydrogen bond and vdW interactions play an important role in the interaction between organic reagents and SS form of tiletamine. The absolute value of λ_2 for hydrogen bond interaction is more than the λ_2 value for the vdW interaction in the case of fumarate, maleate, and succinate that shows the importance of hydrogen bond interaction between organic reagents and the SS form of tiletamine. Also, 3D NCI diagrams confirmed the presence of the N-H...O interaction with hydrogen bond nature between the organic achiral reagents and SS form of tiletamine in agreement with previous results.

Conclusion

According to the results, the interaction energy between SS form of tiletamine and oxalate, succinate, fumarate, and maleate anions is higher than other organic achiral reagents. Therefore, these reagents have a greater capability for conglomerate crystal formation. Likewise, it is demonstrated that with increasing in the length of carbon chain in organic achiral anions (higher than 4 carbon atoms in the adipate, glutarate, suberate, and pimelate anions), the ability of conglomerate formation by organic achiral anions decreased. These results indicate the negative effect of steric barrier of organic achiral anions decreasing the interaction between organic achiral anions with tiletamine. The interaction energy of the organic achiral anions with tiletamine decreased with increasing in the solvent polarity. Finally, the results of this study indicate that computational modeling is a useful method for exploring the possibility of conglomerate formation in the proximity of organic achiral reagents.

Acknowledgements

The authors are grateful for the spiritual support of Imam Hossein University.

Conflict of Interest

We have no conflicts of interest to disclose

Orcid:

Nabi Javadi:

<https://www.orcid.org/0000-0002-7102-9949>

Hossein Fakhraian:

<https://www.orcid.org/0000-0001-8020-6639>

References

- [1] D. Zheng, A. Asano, Biocatalytic asymmetric ring-opening of dihydroisoxazoles: a cyanide-free route to complementary enantiomers of β -hydroxy nitriles from olefins, *Green Chem.*, **2020**, *22*, 4930-4936. [[crossref](#)], [[Google Scholar](#)], [[Publisher](#)]
- [2] L.C. Preiss, L. Werber, V. Fischer, S. Hanif, K. Landfester, Y. Mastai, R. Munoz-Espi, Amino-acid-based chiral nanoparticles for enantioselective crystallization, *Adv. Mater.*, **2015**, *27*, 2728-2732. [[crossref](#)], [[Google Scholar](#)], [[Publisher](#)]
- [3] C. Viedma, J.M. McBride, B. Kahr, P. Cintas, Enantiomer-specific oriented attachment: formation of macroscopic homo-chiral crystal aggregates from a racemic system, *Angew. Chem. Int. Ed.*, **2013**, *52*, 10545-10548. [[crossref](#)], [[Google Scholar](#)], [[Publisher](#)]
- [4] S. Hadidi, F. Shiri, M.S. Norouzbaz, Mechanistic study of fenopropfen photoisomerization to pure (S)-fenopropfen: a DFT study, *Struct Chem.*, **2020**, *31*, 115-122. [[crossref](#)], [[Google Scholar](#)], [[Publisher](#)]
- [5] Y. Kim, J. Park, M.J. Kim, Dynamic kinetic resolution of amines and amino acids by enzyme-metal cocatalysis, *ChemCatChem*, **2011**, *3*, 271-277. [[crossref](#)], [[Google Scholar](#)], [[Publisher](#)]
- [6] Y. Okamoto, T. Ikai, Chiral HPLC for efficient resolution of enantiomers, *Chem. Soc. Rev.*, **2008**, *37*, 2593-2608. [[crossref](#)], [[Google Scholar](#)], [[Publisher](#)]
- [7] K. Shimomura, T. Ikai, S. Kanoh, E. Yashima, K. Maeda, Switchable enantioselective separation based on macromolecular

- memory of a helical polyacetylene in the solid state, *Nat. Chem.*, **2014**, *6*, 429-434. [[crossref](#)], [[Google Scholar](#)], [[Publisher](#)]
- [8] H. Lorenz, A. Seidel-Morgenstern, Processes to separate enantiomers, *Angew. Chem. Int. Ed.*, **2014**, *53*, 1218-1250. [[crossref](#)], [[Google Scholar](#)], [[Publisher](#)]
- [9] J.P.M. Lommerse, W.D.S. Motherwell, H.L. Ammon, A. Gavezzotti, D.W.N. Hofmann, F.F.J. Leusen, W.T.M. Mooij, S.L. Price, B. Schweizer, M.U. Schmidt, M.P. Man Eijck, P. Verwer, D.E. Williams, A test of crystal structure prediction of small organic molecules, *Acta Cryst.*, **2000**, *56*, 697-714. [[crossref](#)], [[Google Scholar](#)], [[Publisher](#)]
- [10] D.D. Medina, J. Goldshtein, S. Margel, Y. Mastai, Enantioselective crystallization on chiral polymeric microspheres, *Adv. Funct. Mater.*, **2007**, *17*, 944-950. [[crossref](#)], [[Google Scholar](#)], [[Publisher](#)]
- [11] R.R. Fayzullin, H. Lorenz, Z.A.A. Bredikhina, A.A. Bredikhina, A. Seidel-Morgenstern, Solubility and some crystallization properties of conglomerate forming chiral drug guaifenesin in water, *J. Pharm. Sci.*, **2014**, *103*, 3176-3182. [[crossref](#)], [[Google Scholar](#)], [[Publisher](#)]
- [12] F. Faigl, E. Fogassy, M. Nogradi, E. Palovicsb, J. Schindlerb, Separation of non-racemic mixtures of enantiomers: an essential part of optical resolution, *Org. Biomol. Chem.*, **2010**, *8*, 947-959. [[crossref](#)], [[Google Scholar](#)], [[Publisher](#)]
- [13] S. Srisanga, J.H. Horst, Racemic compound, conglomerate, or solid solution: phase diagram screening of chiral compounds, *Cryst. Growth Des.*, **2010**, *10*, 1808-1812. [[crossref](#)], [[Google Scholar](#)], [[Publisher](#)]
- [14] D. Kozma, Z. Böcskei, K. Simon, E. Fogassy, Racemic compound formation conglomerate formation. Part. 1. Structural and thermos-analytical study of hydrogen malonate, hydrogen phthalate and hydrogen succinate of α -phenylethylamine, *J. Chem. Soc. Perkin Trans.*, **1994**, *2*, 1883-1886. [[crossref](#)], [[Google Scholar](#)], [[Publisher](#)]
- [15] E. Choobdari, H. Fakhraian, M.H. Peyrovi, Anion effect on the binary and ternary phase diagrams of chiral medetomidine salts and conglomerate crystal formation, *Chirality*, **2014**, *26*, 183-188. [[crossref](#)], [[Google Scholar](#)], [[Publisher](#)]
- [16] M. Khavani, R. Kalantarinezhad, M. Izadyar, A joint QM/MD study on α -, β - and γ -cyclodextrins in selective complexation with cathinone, *Supramol. Chem.*, **2018**, *8*, 687-696. [[crossref](#)], [[Google Scholar](#)], [[Publisher](#)]
- [17] E. Soleymania, H. Alinezhad, M.D. Ganji, M. Tajbakhsh, Enantioseparation performance of CNTs as chiral selectors for the separation of ibuprofen isomers: A dispersion corrected DFT study, *J. Mater. Chem. B*, **2017**, *5*, 6920-6929. [[crossref](#)], [[Google Scholar](#)], [[Publisher](#)]
- [18] N. Javadi, M. Rezaeian, H. Fakhraian, The conglomerate crystal formation of methoxetamine salts in the presence of some organic achiral anions: a theoretical approach, *Supramol. Chem.*, **2021**, *5*, 183-193. [[crossref](#)], [[Google Scholar](#)], [[Publisher](#)]
- [19] V. Zarei, N. Javadi, Z. Ghahramani, H. Fakhraian, Role of hydrogen transfer and ionic bonding on RR, SS and RS medetomidine conglomerates/acids stability: A theoretical Study, *J. Sci.*, **2019**, *30*, 241-250. [[Google Scholar](#)], [[Publisher](#)]
- [20] N. Javadi, M. Aallaei, K. Adib, M. Atifeh, Theoretical Investigations on the Separation of Medetomidine Enantiomers, *Chem. Methodol.*, **2020**, *4*, 788-797. [[crossref](#)], [[Google Scholar](#)], [[Publisher](#)]
- [21] N. Javadi, S. Habibzade, M. Aallaei, K. Adib, S.M. Atife, Feasibility of enantiomeric separation of racemic compounds using a simple method: theoretical investigation of anion ability to conglomerate crystal formation of ketamine salts, *Eurasian Chem. Commun.*, **2020**, *2*, 1050-1058. [[crossref](#)], [[Google Scholar](#)], [[Publisher](#)]
- [22] G. Chen, C.R. Ensor, B. Bohner, The pharmacology of 2-(ethylamino)-2-(2-thienyl)-cyclohexanone-HCl (CI-634), *J.*

- Pharmacol. Exp. Ther.*, **1969**, *168*, 171-179. [[Google Scholar](#)], [[Publisher](#)]
- [23] P. Popik, M. Hołuj, T. Kos, G. Nowak, T. Librowski, K. Sałat, Comparison of the Psychopharmacological Effects of Tiletamine and Ketamine in Rodents, *Neurotox. Res.*, **2017**, *32*, 544-554. [[crossref](#)], [[Google Scholar](#)], [[Publisher](#)]
- [24] K.W. Lee, A.H.E. Hassan, Y. Jeong, S. Yoon, S.H. Kim, C.J. Lee, H.R. Jeon, S.W. Chang, J.Y. Kim, D.S. Jang, H.J. Kim, H.J. Cheonge, Y.S. Lee, Enantiopure methoxetamine stereoisomers: chiral resolution, conformational analysis, UV-circular dichroism spectroscopy and electronic circular dichroism, *New J. Chem.*, **2021**, *45*, 4354-4364. [[crossref](#)], [[Google Scholar](#)], [[Publisher](#)]
- [25] M.J. Frisch, G.W. Trucks, H.B. Schlegel, G.E. Scuseria, M.A. Robb, J.R. Cheeseman, G. Scalmani, V. Barone, B. Mennucci, G.A. Petersson, H. Nakatsuji, M. Caricato, X. Li, H.P. Hratchian, A.F. Izmaylov, J. Bloino, G. Zheng, J.L. Sonnenberg, M. Hada, M. Ehara, K. Toyota, R. Fukuda, J. Hasegawa, M. Ishida, T. Nakajima, Y. Honda, O. Kitao, H. Nakai, T. Vreven, J.E. Peralta, F. Ogliaro, M. Bearpark, J.J. Heyd, E. Brothers, K.N. Kudin, V.N. Staroverov, T. Keith, R. Kobayashi, J. Normand, K. Raghavachari, A. Rendell, J.C. Burant, S.S. Iyengar, M.C. Tomasi, J.M.M. Rega, M. Klene, J.E. Knox, J.B. Cross, C.A. Bakken, Jaramillo, R. Gomperts, O.Y. Stratmann, R. Austin, C.P. Cammi, R.L.M. Ochterski, V.G.Z. Morokuma, G.A. Voth, J.J.D. P Salvador, S. Dapprich, A.D. Daniels, O. Farkas, J.B. Foresman, J.V. Ortiz, J. Cioslowski, D.J. Fox, (2010) Gaussian 09, Revision C.01. Gaussian, Inc., Wallingford.
- [26] S. Grimme, Semiempirical GGA-type density functional constructed with a longrange dispersion correction, *J. Comput. Chem.*, **2006**, *27*, 1787-1799. [[crossref](#)], [[Google Scholar](#)], [[Publisher](#)]
- [27] J. Kona, W.M.F. Fabian, Hybrid QM/MM calculations on the first redox step of the catalytic cycle of bovine glutathione peroxidase GPx1, *J. Chem. Theory Comput.*, **2011**, *7*, 2610-2616. [[crossref](#)], [[Google Scholar](#)], [[Publisher](#)]
- [28] M. Cossi, V. Barone, R. Cammi, J. Tomasi, Ab initio study of solvated molecules: a new implementation of the polarizable continuum model, *Chem. Phys. Lett.*, **1996**, *255*, 327-335. [[crossref](#)], [[Google Scholar](#)], [[Publisher](#)]
- [29] G. Scalmani, M.J. Frisch, Continuous surface charge polarizable continuum models of solvation. I. General formalism, *J. Chem. Phys.*, **2010**, *132*, 114110-114118. [[crossref](#)], [[Google Scholar](#)], [[Publisher](#)]
- [30] A.E. Reed, L.A. Curtiss, F. Weinhold, Intermolecular interactions from a natural bond orbital, donor-acceptor viewpoint, *Chem. Rev.*, **1988**, *88*, 899-926. [[crossref](#)], [[Google Scholar](#)], [[Publisher](#)]
- [31] W. Scherer, P. Sirsch, D. Shorokhov, M. Tafipolsky, G.S. McGrady, E. Gullo, Valence charge concentrations, electron delocalization and β -agostic bonding in d^0 metal alkyl complexes, *Chem. Eu. J.*, **2003**, *9*, 6057-6070. [[crossref](#)], [[Google Scholar](#)], [[Publisher](#)]
- [32] H. Schmider, A. Becke, Chemical content of the kinetic energy density, *J. Mol. Struct.*, **2000**, *527*, 51-61. [[crossref](#)], [[Google Scholar](#)], [[Publisher](#)]
- [33] R. Chaudret, B.D. Courcy, J. Contreras-Garcia, E. Gloaguen, A. Zehnacker-Rentien, M. Mons, J.P. Piquemal, Unraveling non-covalent interactions within flexible biomolecules: from electron density topology to gas phase spectroscopy, *Phys. Chem. Chem. Phys.*, **2014**, *16*, 9876-9891. [[crossref](#)], [[Google Scholar](#)], [[Publisher](#)]
- [34] T. Lu, F. Chen, Multiwfn: a multifunctionalWavefunction analyzer, *J. Comput. Chem.*, **2012**, *33*, 580-592. [[crossref](#)], [[Google Scholar](#)], [[Publisher](#)]
- [35] Jeffrey G.A., An Introduction to hydrogen bonding. Oxford University Press, **1997**. [[Google Scholar](#)], [[Publisher](#)]
- [36] S.D. Muzio, F. Ramondo, F. Gontrani, F. Ferella, M. Nardone, P. Benassi, Choline hydrogen dicarboxylate ionic liquids by x-ray scattering, vibrational spectroscopy and

molecular dynamics: h-fumarate and h-maleate and their conformations, *Molecules*, **2020**, *25*, 4990. [[crossref](#)], [[Google Scholar](#)], [[Publisher](#)]

How to cite this article: Nabi Javadi*, Hossein Fakhraian. Investigation of enantiomeric separation of tiletamine drug using computational chemistry methods. *Eurasian Chemical Communications*, 2023, *5*(7), 661-674. **Link:** https://www.echemcom.com/article_169616.html